

Available online at <https://www.tjnpr.org>*Original Research Article*

Comparative Cytotoxicity and Green Synthesis of Silver Nanoparticles from *Sansevieria cylindrica*

Andhavarapu V S K Bhavani and Annammadevi G Sayam*

Department of Pharmaceutics, Gitam School Of Pharmacy, Visakhapatnam,

ARTICLE INFO**Article history:**

Received 25 July 2024

Revised 28 July 2024

Accepted 05 November 2024

Published online 01 December 2024

ABSTRACT

The synthesis of silver nanoparticles (AgNPs) using phytochemicals is increasingly recognized for its biocompatibility and therapeutic potential. This study explores the green synthesis of AgNPs using *Sansevieria cylindrica* extract and compares their antioxidant activities and cytotoxicity against MCF-7, HeLa, SKOV3 and HUVEC cell lines. The hydroalcoholic extract of *S. cylindrica* was analysed for phytochemical content and AgNP synthesis and characterised by UV-Vis and FT-IR spectroscopy, SEM, zeta potential, and particle size analyzer. The green synthesis of AgNPs was optimized by varying concentrations of AgNO₃ and extract at different temperatures and times. The synthesized NP was confirmed by UV-visible spectrophotometry, with a distinct peak at 425 nm, characteristic of AgNPs. FT-IR analysis revealed the presence of functional groups from the extract that stabilized the nanoparticles. SEM imaging demonstrated mostly spherical nanoparticle sizes (100 nm). Zeta potential analysis indicated moderate stability (-24.3 mV), and particle size analysis revealed a broad distribution, with a dominant population around 127.37 nm and some larger aggregates, suggesting room for optimisation of the synthesis process. The AgNPs exhibited significantly higher cytotoxic effects against the cancer cell lines (MCF-7, HeLa, and SKOV3) than the crude extract, with reduced toxicity towards non-cancerous HUVEC cells. The total phenolic and flavonoid contents were quantified, affirming its antioxidant capacity. The findings suggest that AgNPs synthesised from *S. cylindrica* are more effective and safer for cancer treatment, emphasising the potential of phytochemical-mediated nanoparticle synthesis in medical applications.

Copyright: © 2024 Bhavani *et al.* This is an open-access article distributed under the terms of the [Creative Commons Attribution License](https://creativecommons.org/licenses/by/4.0/), which permits unrestricted use, distribution, and reproduction in any medium, provided the original author and source are credited.

Keywords: *Sansevieria cylindrica*, Silver Nanoparticles, Antioxidant Activity, Cytotoxicity Assay.

Introduction

Cancer is a significant global health issue involving the uncontrolled growth of cells and their ability to spread to different body areas. It covers various diseases that can affect various organ systems and are caused by genetic mutations, environmental influences, lifestyle choices, and chronic infections.¹⁻⁴ Cancer is a complex disease that can outsmart the immune system and resist treatment, making it even more challenging to treat. Cancer is a significant global cause of death, affecting countless lives and taking a toll on society, both economically and emotionally. Despite the progress made in medical science, there is still a pressing need for better and safer treatments to improve survival rates. Driven by this sense of urgency, researchers constantly seek new and innovative treatments.⁵⁻⁷ One promising avenue is the development of targeted therapies that can specifically target cancer cells without harming healthy tissues. This approach holds great promise for improving patient outcomes and quality of life.⁸⁻¹⁰ The quest for novel and effective agents for treating cancer has led to exploring phytochemicals and their derivatives, including nanoparticles synthesised from plant extracts.¹¹

This search is fuelled by the need for treatments that are not only efficacious but also exhibit lower toxicity towards normal cells. Silver nanoparticles (AgNPs) have emerged as a promising avenue in nanomedicine owing to their remarkable properties, such as high surface area and easy functionalisation. These attributes make AgNPs a versatile platform for drug delivery and therapeutic agents.¹² *Sansevieria cylindrica*, from the Asparagaceae family, is known for its upright and cylindrical foliage, which can reach heights of up to 5 feet, showcasing a radial symmetry that distinguishes it from other flora.¹³⁻¹⁵ It is a renowned indoor plant because of its resilience and ease of care, as it can tolerate variable temperatures, low light, and infrequent watering.¹⁶ In addition to its decorative function, *S. cylindrica* has a rich history in traditional medicine, which has been used to alleviate respiratory and gastrointestinal ailments, highlighting its medicinal value. The bioactive components of plants, such as glucuronate substances, cardenolides, polyphenols, and saponins, endow them with antioxidant and antibacterial properties. Its ability to purify air is attributable to the presence of pregnane glycosides and steroids.¹⁷⁻¹⁹ This study addresses a significant gap in the ethnopharmacological knowledge of *Sansevieria cylindrica* by exploring its potential in the green synthesis of silver nanoparticles (AgNPs). While *S. cylindrica* is renowned for its traditional medicinal uses, its application in nanomedicine remains underexplored. By synthesising biocompatible and effective AgNPs from *S. cylindrica*, this research seeks to validate their efficacy and safety, hypothesising that they may offer a superior therapeutic profile compared to conventional treatments. Silver was chosen explicitly over other nanomaterials due to its exceptional antimicrobial and anticancer properties, high surface area, ease of functionalisation, and strong interaction with biological molecules. These attributes make AgNPs an ideal candidate for developing advanced and sustainable cancer therapies, bridging traditional phytochemistry with nanotechnology.

*Corresponding author. E mail: mannam@gitam.edu
Tel: +91 9866396797

Citation: Bhavani AVSK Annammadevi GS. Comparative Cytotoxicity and Green synthesis of Silver Nanoparticles from *Sansevieria cylindrica*. Trop J Nat Prod Res. 2024; 8(11): 9104 – 9110
<https://doi.org/10.26538/tjnpr/v8i11.19>

Official Journal of Natural Product Research Group, Faculty of Pharmacy, University of Benin, Benin City, Nigeria

Materials and Methods

Collection of Plant material

Sansevieria cylindrica was collected from Hyderabad (17.417027926199097, 78.53196134482792), Telangana, in November 2022 and authenticated from the Sri Venkateswara University (Voucher specimen Number-0925).

Extraction Procedure

The plant material (1 kg of the leaf) was pulverized after drying. The powdered material was macerated in hydroalcohol (ethanol: water solution of 70:30 v/v) with frequent stirring and allowed to extract for seven days. The filtrate was concentrated to dryness using a vacuum-stopped rotary evaporator (Vedh Instruments, Hyderabad, India) to obtain the crude extract.²⁰⁻²¹

Qualitative Phytochemical Analysis

Preliminary phytochemical analysis of the *S. cylindrica* leaf extracts was performed according to established protocols.²²

Quantitative Phytochemical Screening

Determination of total phenolic content

The modified Singleton method was used to determine the total phenolic content of *S. cylindrica*. A gallic acid stock solution was prepared and diluted with ethanol to different concentrations (25–100 µg/mL). After adding 10% Folin-Ciocalteu reagent to 7.5% w/v sodium carbonate, the mixture was incubated at room temperature for two hours. Absorbance was measured at 765 nm using a UV-visible spectrophotometer (Shimadzu-1800, Japan) in triplicate. The total phenolic content was reported as milligrams of gallic acid equivalents (GAE) per gram of sample in dry weight (mg/g) after a calibration curve was created.²³⁻²⁴

Determination of total flavonoid content

The Dowd method was used to quantify the total flavonoid content in *S. cylindrica*. A volume of 0.2 mL of 10% (w/v) aluminium chloride solution, 0.2 mL of 1 M potassium acetate, and distilled water were combined with 1 mL of a sample solution that included plant extracts and quercetin. After incubating the mixture for 30 minutes, a UV-visible spectrophotometer operating in triplicate at a wavelength of 415 nm was used to measure the absorbance. The findings are reported in milligrams per gram (mg QE/g), with the results as mg quercetin equivalents per gram of dry extract.²⁵⁻²⁶

In vitro antioxidant activity study

DPPH assay

DPPH radical scavenging experiments were performed to evaluate the ability of the ethanolic extracts of *S. cylindrica* to scavenge free radicals. After mixing 0.2 mL of the extract solution with 2 mL of a 0.5 mM DPPH solution. The reference standard was ascorbic acid, and the absorbance of each extract was measured thrice at 515 nm after 20 min of incubation.²⁷ The antioxidant activity was calculated using the following formula (1):

$$\% \text{ inhibition} = \frac{\text{Absorbance of the Control} - \text{Absorbance of Test}}{\text{Absorbance of the Control}} \times 100 \quad (1)$$

Nitric oxide radical scavenging assay

The ability of *S. cylindrica* extracts to scavenge nitric oxide radicals was tested by combining the extract (0.5 mL) with 2 mL of a 10 mM solution of sodium nitroprusside and 0.5 mL (pH 7.4) and incubating the mixture at 25°C for 150 min.²⁸ After the incubation the readings were noted for the blank (dimethyl sulfoxide), standard (Ascorbic acid), and test (*S. cylindrica* extracts) samples at 540nm, and the percentage of NO inhibition was calculated using Formula 1.

Cytotoxicity Assay

The cytotoxic activity of *S. cylindrica* was assessed using the MTT assay. Cancer cell lines (ATCC), including cervical (HeLa), breast (MCF-7), ovarian (SKOV3), and human umbilical vein endothelial cells (HUVECs), were selected for the study. These cells were cultured in 96-well plates under standard controlled conditions, for 72 hours. After incubation, MTT reagent (20 µL of 2 mg/mL in phosphate-buffered saline) was added to each well, and the cells were incubated for an additional 3 hours. Mitochondrial enzymes within the viable cells reduced the MTT, resulting in the formation of purple formazan crystals. These crystals were dissolved in 100 µL of DMSO, and the optical density of the solution was measured at 540 nm in triplicate using a spectrophotometer. The absorbance values, which reflect cell viability, were used to determine the IC₅₀ value—the concentration needed to inhibit 50% of cell viability. These IC₅₀ values were then compared with those of the standard chemotherapeutic agent Doxorubicin and blank controls.²⁹

Green synthesis of AgNps

A mixture of silver nitrate (AgNO₃) solution and the various concentrations of test solutions were made and allowed to react under various experimental conditions. Different concentrations of the *S. cylindrica* extract (0.10 to 1.00%) and silver nitrate (0.5 mM to 10 mM). The combinations were allowed to react for 15, 30, 60, 90, and 120 minutes at varying temperature conditions (25°C to 100°C). After the reaction, the mixtures were subjected to cold centrifugation for 15 minutes at 11,000 rpm. The pellets were thoroughly washed with deionized water multiple times to ensure purity and then dried in an oven at 50°C for further analysis. The most efficient and stable conditions identified during these experiments were subsequently applied for the bulk production of AgNPs, highlighting their rapid ion reduction and stabilisation properties.³¹

Characterization of AgNPs

To characterise the synthesised silver nanoparticles (AgNPs), a range of analytical techniques was utilized:

Ultraviolet-visible (UV-Vis) spectroscopic analysis

Initially, Ultraviolet-visible (UV-Vis) spectroscopy was employed to evaluate the optical properties of the AgNPs. For this purpose, 3 mL of the AgNP solution was analyzed at room temperature (25°C). The absorbance spectra were recorded across a wavelength range of 200–800 nm with a 1 nm resolution, adhering to standard procedures.

FT-IR Analysis of AgNPs

Fourier Transform Infrared (FT-IR) spectroscopy was conducted (BRUKER OPTICS TENSOR 27 model Germany) to determine the functional groups associated with the nanoparticles. The FT-IR spectra were acquired over the range of 600 to 4000 cm⁻¹, with a transmittance resolution of 5 cm⁻¹.

Scanning Electron Microscopic Analysis

For morphological analysis, Field Emission Scanning Electron Microscopy (FESEM) was performed using a FEI Apreo LoVac model, which is equipped with a “retractable STEM 3+ Detector and DBS Detector”. The AgNP samples were adhered to “carbon conductive tape” to ensure stability and obtain high-resolution images.

Particle size analysis

Additionally, the particle size, volume, and distribution were assessed using a particle size analyzer, providing detailed insights into the physical characteristics of the nanoparticles.³²

Statistical analysis

Microsoft Excel with appropriate formula tools was used as needed.

Results and Discussions

The phytochemicals detected in the leaf extract of *S. cylindrica* are presented in Table 1. Alkaloids and tannins are reducing agents, aiding in the transformation of silver ions (Ag^+) into nanoparticles. Terpenoids including Saponins reduce the silver ions and stabilise the AgNPs. Carbohydrates help to prevent the aggregation of the AgNPs. The combined action of these phytochemicals leads to the efficient synthesis and stabilisation of AgNPs, making them well-suited for a range of applications (Table 1).³³⁻³⁴ The total phenolic content was assessed using the "Folin-Ciocalteu method" with gallic acid as the standard (Table 2) and was observed as 75.86 ± 0.14 mgGE/g. The flavonoid content was measured as 12.17 ± 0.78 mg of gram equivalence of quercetin (mg QE/g) at 415 nm (Table 2).

S. cylindrica demonstrated significant DPPH radical scavenging activity in a dose-dependent manner compared to ascorbic acid in the present study (Table 3). At a higher concentration of $75 \mu\text{g/mL}$, the extract exhibited 41.8% inhibition ($\text{IC}_{50} = 81.34 \mu\text{g/mL}$), which was second only to ascorbic acid (79.97%; $\text{IC}_{50} = 39.42 \mu\text{g/mL}$). These results suggested that the plant possesses potent antioxidant (Figure 1) properties. As shown in Figure 2, *S. cylindrica* exhibited notable nitric oxide radical scavenging activity, which was dose-dependent. At a higher concentration of $75 \mu\text{g/mL}$, the extract showed a significant inhibition of 39.5%, with IC_{50} values of $90.55 \mu\text{g/mL}$. These results indicate that the extract possesses potent antioxidant properties, combating oxidative stress and offering potential protective effects in the body.

Table 1: Qualitative phytochemical study of *S. cylindrica*

Phytochemical	Present (+) / Absent (-)
Alkaloids	+
Glycosides	-
Flavonoids	+
Terpenoids&steroids	+
Saponins	+
Tannins	-

(+) Present, (-) Absent

Table 2: Quantitative phytochemical study of *S. cylindrica*

Quantitative phytochemical study	Result
Total phenolic content	75.86 ± 0.14 mgGE/g
Total flavonoid content	12.17 ± 0.78 mgQE/g

*All values are expressed as Mean \pm SD for three determinations"

Table 3: Percentage inhibition and IC_{50} values at different concentrations of standard Ascorbic acid with *Sansevieria cylindrica* extract

Concentration $\mu\text{g/mL}$	DPPH assay		NO free radical assay	
	Ascorbic acid	<i>S. cylindrica</i>	Ascorbic acid	<i>S. cylindrica</i>
75	92.68 ± 0.25	83.29 ± 0.22	86.63 ± 0.33	81.98 ± 0.44
50	74.95 ± 0.12	69.00 ± 0.63	66.06 ± 0.25	57.28 ± 0.65
25	68.74 ± 0.22	60.20 ± 0.14	47.15 ± 0.34	40.64 ± 0.21
15	60.17 ± 0.14	57.15 ± 0.22	51.33 ± 0.61	45.55 ± 0.68
10	46.39 ± 0.35	38.63 ± 0.14	36.34 ± 0.45	28.80 ± 0.74
$\text{IC}_{50} \mu\text{g/ml}$	$21.65 \mu\text{g/ml}$	$27.58 \mu\text{g/ml}$	$31.38 \mu\text{g/ml}$	$37.61 \mu\text{g/ml}$

To optimise the synthesis of nanoparticles, a range of AgNO_3 concentrations was tested in combination with varying amounts of *S. cylindrica* leaf extract under different temperatures and time intervals. Notably, after 60 minutes, the reaction involving a 0.2% concentration of the test sample with 1 mM AgNO_3 (40°C) led to the formation of

AgNPs that can be observed visually with the transformation of yellow to brown colouration, which is an indication of reduction of silver cation to its metallic form, indicating efficient nanoparticle formation. The successful synthesis of silver nanoparticles (AgNPs) in solution was confirmed using UV-visible spectrophotometry (Figure 3), which identified a Surface Plasmon Resonance (SPR) absorption band within the 430-436 nm wavelength range. The spectral analysis included the newly synthesized AgNPs, silver nitrate, and the *S. cylindrica* extract. A distinct absorption peak at 425 nm, characteristic of AgNPs, was observed. SPR band at 425 nm, typically indicates the presence of smaller, spherical nanoparticles. In contrast, multiple SPR bands at longer wavelengths would suggest the presence of big, uneven nanoparticles. The symmetry of the observed SPR band further indicated the absence of significant particle aggregation in the solution.

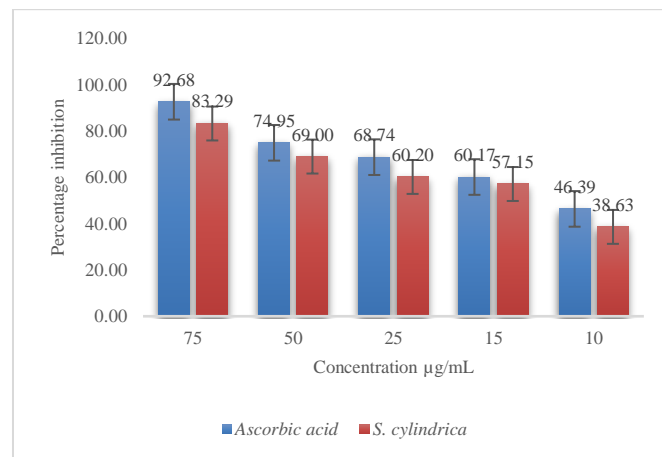


Figure 1: Effect of *S. cylindrica* on DPPH radicals

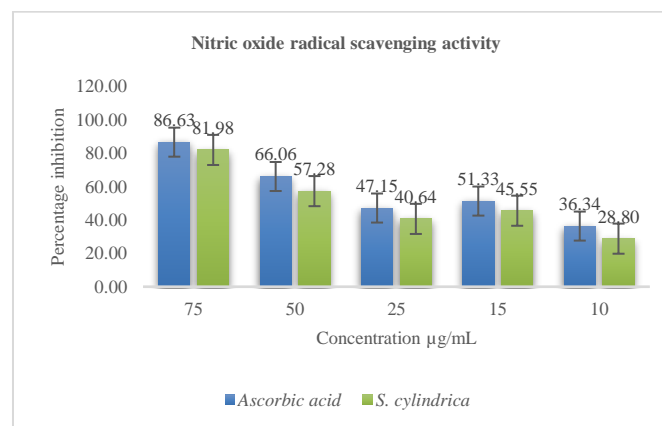


Figure 2: Effect of *S. cylindrica* on NO radicals

Therefore, the sharp, symmetric peak at 425 nm confirms the successful production of small-spherical AgNPs with minimal agglomeration. Similarly, FT-IR analysis of the *S. cylindrica* extract revealed distinct absorption bands corresponding to various functional groups, highlighting the phytochemical composition of the extract. A broad, prominent band around 3300 cm^{-1} indicates hydroxyl (OH-) groups of alcohol, phenol, and flavonoids, which are known to act as stabilising agents on the nanoparticle surface. Additionally, a band at 1627 cm^{-1} corresponds to carbon double bonds, typical of rigid skeleton systems of compounds. The carboxylic acid groups can be assigned to the peaks at 1151 cm^{-1} and 1014 cm^{-1} . Furthermore, the detection of bands at 904 cm^{-1} points to the presence of unsaturated bonds in aromatic compounds. The phytochemicals present in the extracts interacted with the metal ions and this change of wavelength can be seen in the spectra which are possibly due to either metallic or redox reactions, ultimately leading to the generation of AgNPs. In addition, these phytochemicals are not only involved in the formation of AgNPs, but also their durability with size uniformity, and individuality (Figure 4a and 4b).

The presence of AgNPs exhibits diverse aggregation patterns characterised by particles of different shapes and sizes. The predominant morphology observed was spherical, with magnifications ranging from 10,000 \times to 40,000 \times . The acquired images provide visual evidence of particles exhibiting a wide range of sizes, encompassing individual nanoparticles measuring approximately 100 nm in diameter alongside larger aggregates that appear to fall within the micrometre scale. This observation supports the previously determined polydispersity index of 21.6% obtained from the analysis of the particle size data. Surface roughness and non-uniform spatial distribution were observable in the observed samples. Notably, dense clustering was observed in certain regions, indicating the possibility of variation in the synthesis or post-synthesis treatment. Scanning electron microscopy (SEM) revealed the existence of nano-sized particles that possess dimensions suitable for applications requiring small sizes. Additionally, larger aggregates were observed, which could influence the colloidal stability and functional performance of the silver nanoparticles (Figure 5). The Zeta potential results revealed a mean zeta potential of -24.3 mV, indicating that the nanoparticles possessed a moderate negative charge. Despite falling below the ± 30 mV threshold, commonly linked to strong colloidal stability, this value suggests a moderate level of stability, with the possibility of some aggregation. The Zeta potential measurements exhibited a relatively low standard deviation of 4.2 mV, indicating a consistent surface charge across the particles in the sample. All the measured particles fell into a single peak (-24.3 mV), which further confirmed the consistent distribution of the surface charge. The Zeta deviation of 11.3 mV demonstrates a reasonable spread of values, suggesting a certain level of variability but generally falling within an acceptable range. In addition, the low conductivity of the suspension (0.0897 mS/cm) indicated that the low ionic strength of the medium did not effectively shield the surface charges. This enabled more precise measurements of zeta potential. Based on these findings, the stability of AgNPs appeared to be moderate. However, modifying the surface chemistry or suspension medium may be beneficial to improve stability and prevent aggregation (Figure 6). The analysis of silver nanoparticles (AgNPs) demonstrated a hydrodynamic diameter of 532.6 nm, accompanied by a polydispersity index (PDI) of 21.6%. This PDI value suggested a wide range of particle sizes, indicating a broad size distribution. The analysed sample exhibited a dominant population of particles with an average diameter of 127.37 nm, constituting approximately 86.75% of the overall distribution. A secondary peak was also observed at 1598.8 nm, representing approximately 13.25% of the total particle population. These findings indicate the potential existence of aggregates. The obtained mean scattering intensity of 125.7 k counts/s and the measured diffusion coefficient of 0.9 $\mu\text{m}^2/\text{s}$ provide evidence of larger particles or aggregates within the sample (Table 4a & 4b). Additionally, the observed transmittance of 83.2% suggests that a significant amount of light can pass through the sample. The observed variability in the size of nanoparticles may have significant implications for their properties and potential applications. This underscores the importance of developing optimized synthesis or processing conditions to ensure a more homogeneous distribution (Figure 7).

Table 4a: Particle size distribution peaks (intensity) of synthesized silver nanoparticles of *Sansevieria cylindrica*

Peak name	Size [nm]	Area [%]	Standard deviation [nm]
Peak 1	127.37	86.75	38.91
Peak 2	1598.8	13.25	411.9
Peak 3	-	-	-

Table 4b: Particle size distribution Parameters of Synthesized silver nanoparticles of *Sansevieria cylindrica*

Parameter	Value
Hydrodynamic diameter	532.6 nm
Mean intensity	125.7 k counts/s
Polydispersity index	21.60%
Absolute intensity	2934.4 k counts/s
Diffusion coefficient	0.9 $\mu\text{m}^2/\text{s}$
Intercept $g1^2$	0.7216
Transmittance	83.20%
Baseline	1.073

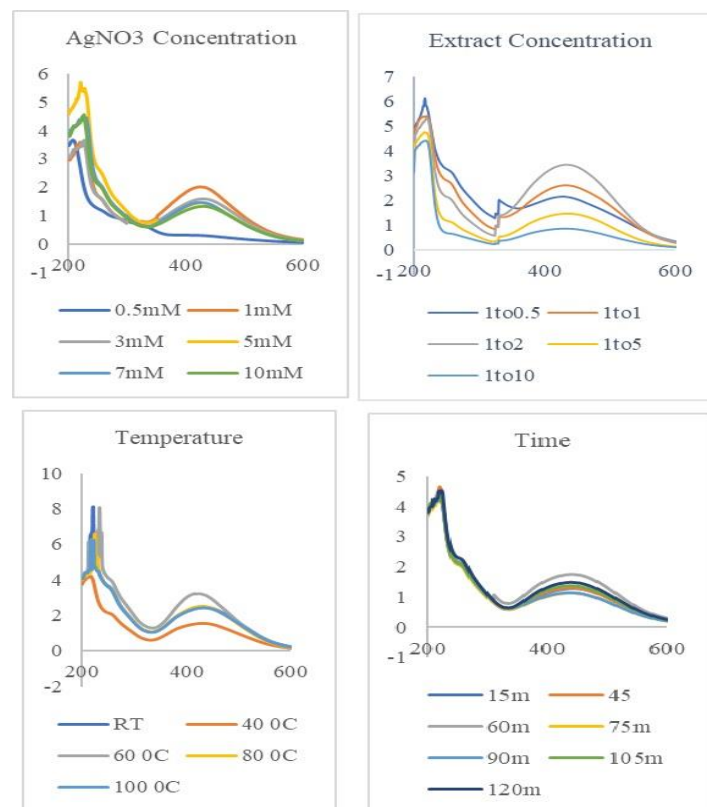


Figure 3: UV spectrophotometric method for optimized silver nanoparticles at lambda max 425nm at different process parameters

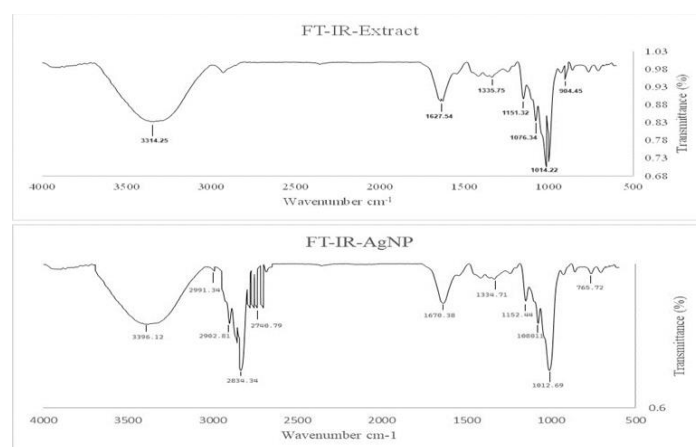


Figure 4: FT-IR spectral data 4a) Hydroalcoholic extract of *Sansevieria cylindrica* 4b) Synthesized silver nanoparticles of *Sansevieria cylindrica*

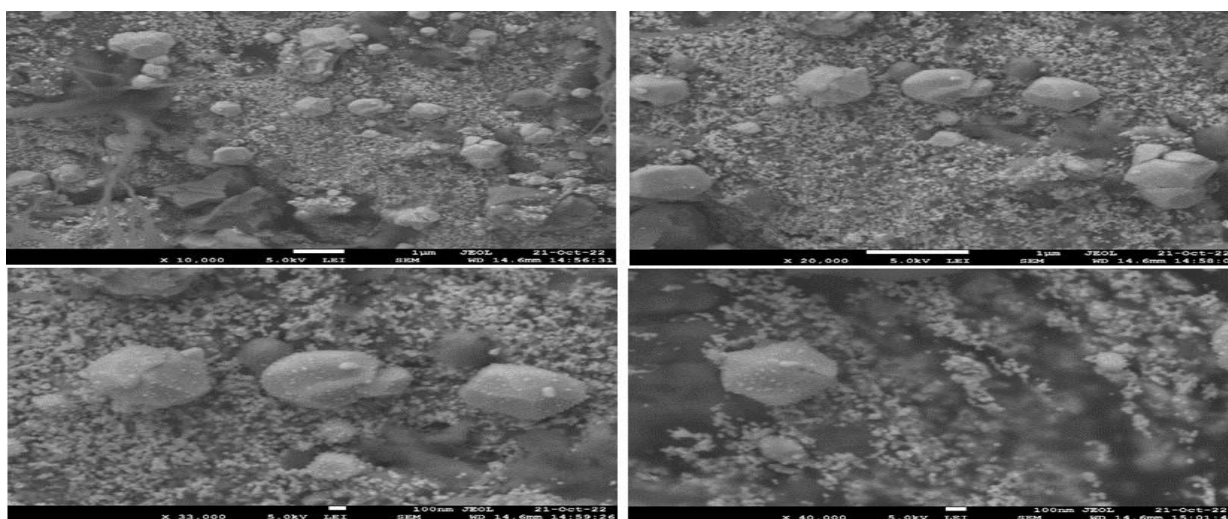


Figure 5: SEM analysis of synthesized silver nanoparticles of *Sansevieria cylindrica* at different magnifications x10000, x20000, x33000, x40000

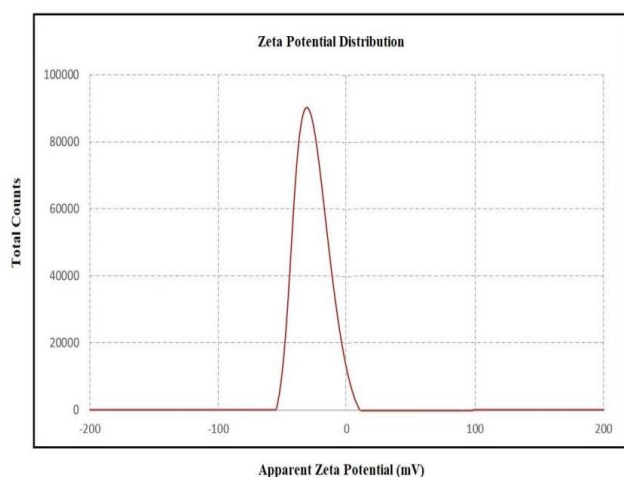


Figure 6: Zeta potential of synthesized AgNPs of Hydroalcoholic extract of *Sansevieria cylindrica*

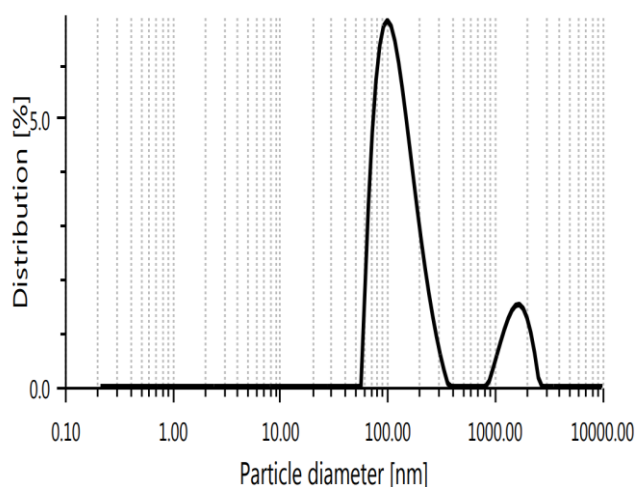


Figure 7: Particle size analysis of synthesized silver nanoparticles of hydroalcoholic extract of *Sansevieria cylindrica*

In the MTT cytotoxicity assay, it was observed that the efficacy of both the *S. cylindrica* extract and AgNPs derived from it varied among different cell lines. In the case of breast cancer (MCF-7), the IC₅₀ values were determined to be 4.81±1.05 µg/mL for *S. cylindrica* and slightly lower at 4.67±1.22 µg/mL for AgNPs. These results suggest that both *S. cylindrica* and AgNPs exhibit comparable potencies against breast cancer cells. An appreciable disparity was noted in the response of cervical cancer (HeLa) cells to the extract and AgNPs. The extract demonstrated a notably higher IC₅₀ value of 21.23±1.67 µg/mL, in contrast to the lower IC₅₀ value of 5.46±1.34 µg/mL observed for AgNPs. The observed trend of enhanced efficacy with silver nanoparticles (AgNPs) persisted in the context of ovarian cancer (SKOV3) cells, with measured values of 15.27±1.36 µg/mL for the extract and 6.38±1.67 µg/mL for AgNPs. Nevertheless, it is worth noting that when tested on non-cancerous HUVEC, both the extract and AgNPs exhibited higher IC₅₀ values. Specifically, the extract displayed an IC₅₀ value of 283.20±1.05 µg/mL, while AgNPs showed an IC₅₀ value of 57.95±1.33 µg/mL (Table 5 and Figure 8). These findings suggest that both the extract and AgNPs have lower toxicity towards normal cells. The findings of this study highlight the considerable potential of silver nanoparticles (AgNPs) as a promising therapeutic agent that surpasses the efficacy of the parent extract, particularly in combating cancer cells. Importantly, this enhanced therapeutic effect was achieved while concurrently minimizing toxicity to non-cancerous cells

Table 5: Comparison between IC₅₀ values of *S. cylindrica* extract and synthesized silver nanoparticles from extract of *S. cylindrica* and Doxorubicin in MTT assay against MCF7, HeLa, SKOV3, HUVEC cell lines

Cell lines	<i>S. cylindrica</i>	AgNPs	Doxorubicin
Breast (MCF7)	4.81±1.05	4.67±1.22	0.0569±0.98
Cervical (HeLa)	21.23±1.67	5.46±1.34	0.1546±0.78
Ovarian (SKOV3)	15.27±1.36	6.38±1.67	0.142±0.25
Human Umbilical Vein Endothelial Cells (HUVEC)	283.20±1.05	57.95±1.33	2.772±0.103

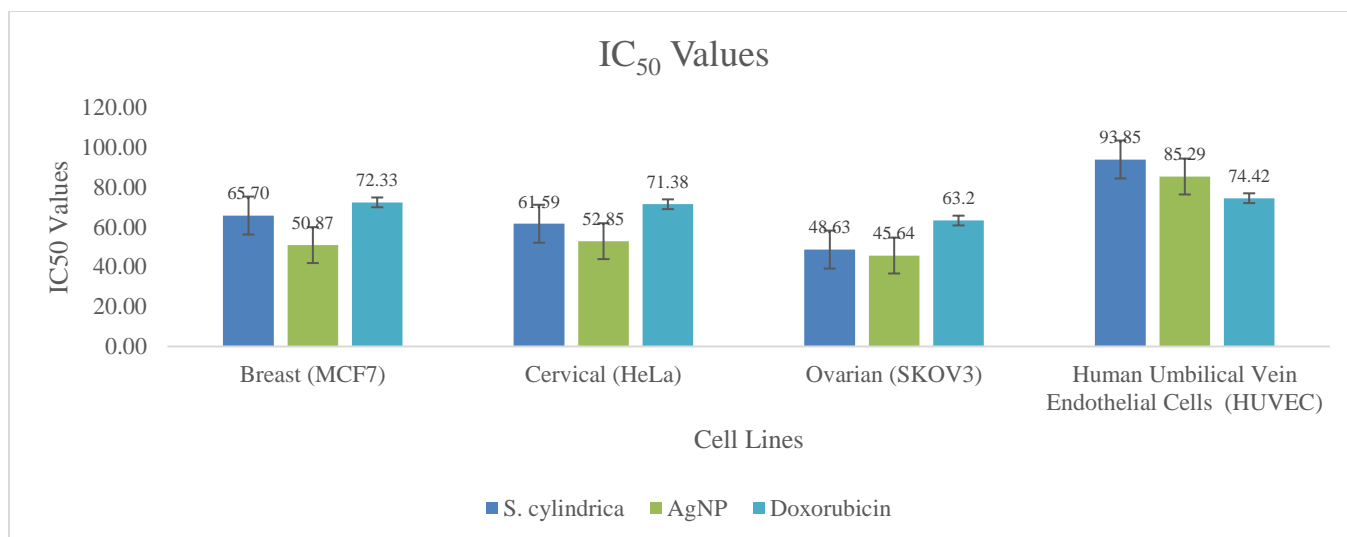


Figure 8: MTT assay results of *Sansevieria cylindrica* extract, synthesized silver nanoparticles from *Sansevieria cylindrica* and Doxorubicin against MCF7, HeLa, SKOV3, HUVEC cell lines

Conclusion

The study on *S. cylindrica* leaf extract has indicated diversified phytochemicals which contribute to the green synthesis of AgNPs. Quantitatively, the total phenolic and flavonoid contents were substantial and may have influenced the antioxidant activities of the extract in the DPPH and nitric oxide radical scavenging assays. For AgNP green synthesis, optimal conditions were identified, leading to the successful formation of nanoparticles, as confirmed by the SPR band and supported by FTIR spectra showing shifts in specific functional groups due to redox interactions. SEM analysis unveiled a diverse morphology of AgNPs with a polydispersity index which suggests a broad size distribution with particles in the normal range. The zeta potential test implied moderate colloidal stability and particle size analysis highlighted the heterogeneity in nanoparticle dimensions. The AgNPs showed enhanced cytotoxic effectiveness over the extract against all the cancer cell lines with the most significant variance against HeLa cells. Both the extract and AgNPs demonstrated lower toxicity towards non-cancerous HUVEC cells. The study on *S. cylindrica* and its derived silver nanoparticles (AgNPs) demonstrates their potential in cancer therapy. The extract facilitates the eco-friendly synthesis of AgNPs, which exhibit higher cytotoxicity against various cancer cell lines while maintaining lower toxicity towards non-cancerous cells compared to the extract alone. SEM and zeta potential analyses confirm the nanoparticles' size consistency and stability, supporting their clinical application potential. Overall, this research underscores the therapeutic promise of plant-mediated AgNPs, advocating for further studies to optimize their synthesis and explore their mechanisms of action in cancer treatment.

Conflict of Interest

The authors declare no conflict of interest.

Authors' Declaration

The authors hereby declare that the work presented in this article is original and that any liability for claims relating to the content of this article will be borne by them.

References

- Blackadar CB. Historical review of the causes of cancer. *World J Clin Oncol.* 2016; 7(1):54-86.
- Parsa N. Environmental factors inducing human cancers. *Iran J Public Health.* 2012; 41(11):1-9.
- Sujatha E, Meraj F. Phytochemical profile, antioxidant and cytotoxic activities of aquatic weed *Landoltia punctata* (G. Mey.) Les & D.J. Crawford. *Ann Phytomed.* 2023; 12(1):1-6. <http://dx.doi.org/10.54085/ap.2023.12.1.33>.
- Pravalika K, Sujatha E. Phytochemical investigation, antioxidant and cytotoxic potential of *Dracaena reflexa* Lam. *Int J Biol Pharm Allied Sci.* 2021; 10(9):698-708. <http://dx.doi.org/10.31032/IJBPAS/2021/10.9.1054>.
- Muz B, Puente P, Azab F, Azab AK. The role of hypoxia in cancer progression, angiogenesis, metastasis, and resistance to therapy. *Hypoxia (Auckl).* 2015; 11(3):83-92. doi: 10.2147/HP.S93413.
- Gao X, Liu J, Cho KB, Kedika S, Guo B. Chemopreventive agent 3,3'-Diindolylmethane inhibits MDM2 in colorectal cancer cells. *Int J Mol Sci.* 2020; 21(13):4642. <https://doi.org/10.3390/ijms21134642>.
- Siegel RL, Miller KD, Wagle NS, Jemal A. Cancer statistics 2023. *CA Cancer J Clin.* 2023; 73:17-48.
- Nikolaou V, Stratigos AJ. Adjuvant treatment in advanced melanoma: How far have we come? *J Eur Acad Dermatol Venereol.* 2023; 37(5):851-852. doi: 10.1111/jdv.19010.
- Usman M, Khan WR, Yousaf N, Akram S, Murtaza G, Kudus KA, Ditta A, Rosli Z, Rajpar MN, Nazre M. Exploring the phytochemicals and anticancer potential of the members of Fabaceae family: A comprehensive review. *Molecules.* 2022; 27(12):3863. doi: 10.3390/molecules27123863.
- Venugopal S, Sudheer KD, Nilanjana B, Ashish K, Tulika C. Phytochemical investigation and antimutagenic potential of ethanolic extracts of *Emblca officinalis*, *Terminalia chebula* and *Terminalia bellirica*. *Nat Prod J.* 2019; 9(1):1-7.
- Vijayan R, Joseph S, Mathew B. *Indigofera tinctoria* leaf extract mediated green synthesis of silver and gold nanoparticles and assessment of their anticancer, antimicrobial, antioxidant and catalytic properties. *Artif Cells Nanomed Biotechnol.* 2018; 46(4):861-871. doi: 10.1080/21691401.2017.1345930.
- Padalia H, Chanda S. Synthesis of silver nanoparticles using *Ziziphus nummularia* leaf extract and evaluation of their antimicrobial, antioxidant, cytotoxic and genotoxic potential (4-in-1 system). *Artif Cells Nanomed Biotechnol.* 2021; 49(1):354-366. doi: 10.1080/21691401.2021.1903478.
- Raslan MA, Melek FR, Said AA, Elshamy AL, Umeyama A, Mounier MM. New cytotoxic dihydrochalcone and steroidal saponins from the aerial parts of *Sansevieria cylindrica* Bojer ex Hook. *Phytochem Lett.* 2017; 22:39-43.

14. Shewale S, Undale V, Bhalchim V, Desai S, Shelar M, Padole S, Chitlange S, Wawale V, Parekh S, Pujari P. Evaluation and assessment of the acute toxic potential of *Sansevieria cylindrica* and *Plumeria obtusa* plant extracts in Wistar albino rats. *J Nat Remedies*. 2022; 22(2):209–220. <https://doi.org/10.18311/jnr/2022/28768>.
15. Dewatisari WF, To'bungan N. Biological activity and phytochemistry of *Dracaena angolensis* Welw. ex Carrière. *Plant Sci Today*. 2023; 10(4):206-214.
16. Aye MM, Aung HT, Thu ZM, Sein MM, Takaya Y, Komori Y, Clericuzio M, Vidari G. Constituents of the rhizomes of *Sansevieria cylindrica*. *Nat Prod Commun*. 2018; 13:1129-1132. doi: 10.1177/1934578X1801300908.
17. Aung HT, Aye MM, Thu ZM, Komori Y, Sein MM, Vidari G. Bioactive constituents from the rhizomes of *Sansevieria cylindrica*. *Rec Nat Prod*. 2020; 14:269-275. doi: 10.25135/rnp.160.19.10.1440.
18. Tanveer A, Singh ND, Khan MF. Phytochemical analysis, total phenolic content of *Sansevieria cylindrica* leaves extract. *Herb Med*. 2017; 3(2):1-6.
19. Ahamad T, Singh D, Khan MF. Phytochemical analysis, total phenolic content, antioxidant and antidiabetic activity of *Sansevieria cylindrica* leaves extract. *J Nat Prod Resour*. 2017; 3(2):134–6. <https://doi.org/10.21767/2472-0151.100026>.
20. Mahalakshmi TV, Sujatha E, Ramadevi B. Total phenolic content, flavonoid content, and antioxidant activity of *Alternanthera ficoidea* (L.) P. Beauv. *Int J Biol Pharm Allied Sci*. 2021; 10(9):453-460.
21. Saidulu A, Sujatha E, Jhansi RG, Karunakar S. Investigating *Cocculus hirsutus* and *Calycopteris floribunda* for antioxidant and antiulcer therapy: A comparative study. *Bull Environ Pharmacol Life Sci*. 2023; 12(4):122-126.
22. Harborne JB. *Phytochemical methods*. Chapman Hall, London New York. 1984; pp. 49-188.
23. Aryal S, Baniya MK, Danekhu K, Kunwar P, Gurung R, Koirala N. Total phenolic content, flavonoid content and antioxidant potential of wild vegetables from Western Nepal. *Plants*. 2019; 8(496).
24. Sudheer KD, Rama MRT. Antioxidant and nephroprotective activity of flavonoid-rich fraction of *Alphonsea sclerocarpa* Thw. *Int J Pharm Sci Drug Res*. 2021; 13(4):384-394.
25. Abbagoni S, Edupuganti S, Rani G. Phytochemical and antioxidant screening of *Cocculus hirsutus* and *Calycopteris floribunda*. *Int J Health Sci*. 2021; 5(S1):576–584. <https://doi.org/10.53730/ijhs.v5nS1.13642>.
26. Sudheer KD, Rama MRT. Antioxidant activity and hepatoprotective potential of flavonoid-rich content of *Alphonsea sclerocarpa* leaves. *Int J Pharm Res*. 2021; 13(3):1309-1318.
27. Alam MN, Bristi NJ, Rafiquzzaman M. Review on in vivo and in vitro methods evaluation of antioxidant activity. *Saudi Pharm J*. 2013; 21(2):143-152.
28. Marcocci JJ, Marguire MT, Droy-lefaiz L. The nitric oxide scavenging properties of *Ginkgo biloba* extract. *Biochem Biophys Res Commun*. 1994; 201:748-755.
29. Ala AA, Olotu BB, Ohia CMD. Assessment of cytotoxicity of leaf extracts of *Andrographis paniculata* and *Aspilia africana* on murine cells in vitro. *Arch Basic Appl Med*. 2018; 6(1):61-65.
30. Sowmya T, Vijaya LG. Spectroscopic investigation on catalytic and bactericidal properties of biogenic silver nanoparticles synthesized using *Soymida febrifuga* aqueous stem bark extract. *J Environ Chem Eng*. 2018; 6(3):3590-3601. <http://dx.doi.org/10.1016/j.jece.2017.01.045>.
31. Johnson H, Joy Prabu. Green synthesis and characterization of silver nanoparticles by leaf extracts of *Cycas circinalis*, *Ficus amplissima*, *Commelina benghalensis* and *Lippia nodiflora*. *Int Nano Lett*. 2015; 5:43–51. <http://dx.doi.org/10.1007/s40089-014-0136-1>.
32. Devadiga A, Shetty KV, Saidutta MB. Timber industry waste-teak (*Tectona grandis* Linn.) leaf extract mediated synthesis of antibacterial silver nanoparticles. *Int Nano Lett*. 2015; 5:205–214. <http://dx.doi.org/10.1007/s40089-015-0157-4>.
33. Kordy MGM, Abdel-Gabbar M, Soliman HA, Aljohani G, BinSabt M, Ahmed IA, Shaban M. Phyto-capped Ag nanoparticles: Green synthesis, characterization, and catalytic and antioxidant activities. *Nanomaterials (Basel)*. 2022; 12(3):373. doi: 10.3390/nano12030373.
34. Callegari A, Tonti D, Chergui M. Photochemically grown silver nanoparticles with wavelength-controlled size and shape. *Nano Lett*. 2003; 3:1565–1568. doi: 10.1021/nl034757a.